Physica Scripta. Vol. 48, 586–592, 1993

Intercombination and Resonance Transitions in the Zn Sequence: Problems in Experiment and Theory

E. Träbert

Experimentalphysik III, Ruhr-Universität Bochum, D-44870 Bochum, Germany

and

L. J. Curtis

Department of Physics and Astronomy, The University of Toledo, Toledo OH 43606, U.S.A.

Received April 2, 1993; accepted in revised form June 8, 1993

Abstract

Beam-foil lifetime data on the intercombination line $4s^2\,{}^1S_0$–$4s4p\,{}^3P_1^\circ$ in the Zn-like ions are reviewed and compared to various theoretical predictions. These predictions spread by about a factor of three. After massive corrections for experimental term energies and singlet-triplet splittings, this spread is reduced to a much narrower band, and most of the predictions then agree with the experimental lifetime findings and with the trend predicted by calculations which explicitly take core polarization into account. A screening parameterization of the experimental lifetime and term structure data can then be used to represent singlet and triplet resonance level lifetimes by a single, common curve.

1. Introduction

Intercombination transitions result from multiplet mixing by the spin-orbit interaction. They find direct applications in plasma diagnostics where their lower decay rate, compared to that of spin-conserving transitions between states of the same electronic configurations, is exploited [1–3]. Fast-ion beam spectroscopy presently offers the only means to measure the rates of such intercombination transitions in highly charged atoms [4]. The theoretical treatment of such transitions is relatively easy in two-electron systems. If, however, there is an electron core, it will be necessary to find out to what extent this can be treated as a closed shell and how much the excitation of this core has to be taken into account. The latter is often called core polarization. One such example is the Zn I isolectronic sequence, with two electrons outside the closed (and completely filled) $n = 3$ shell. In the following, the resonance and intercombination lines in this sequence are discussed as a challenging example: the many-electron core presents a test case for the theoretical treatment of core-polarization, and a number of experimental data are available to check on the theoretical results.

In a recent series of three papers, Huang and coworkers presented theoretical data (energies and oscillator strengths) on the resonance and intercombination transitions in three homologous sequences (Zn, Cd, Hg) [5–7] and compared their results with beam-foil data, finding poor agreement. Conceding that their own calculations lacked a proper treatment of core polarization effects, they nevertheless put the blame for the claimed discrepancies on the experiments, in particular on the cascade problem in beam-foil spectroscopy. As has already been demonstrated in detail by Pinnington and Baylis in a Comment [8] on the Hg sequence paper of the above series, Huang *et al.* mostly compared their results with outdated experimental results and overlooked the more recent literature which contains better and rather more reliable data, from improved measurements and evaluation techniques. Furthermore, Pinnington and Baylis could show that core polarization makes all the difference. When this is allowed for, theoretical data and experimental results in the Hg sequence do in fact agree.

For the Zn sequence, Hibbert a few years ago already indicated the necessity of taking core polarization into account [9], and more recently Hibbert and Bailie [10] strengthened this point by explicit examples: They point out the insufficient treatment or even neglect of these core-polarization effects in most calculations of the Zn I sequence, and they indicated the type and estimated the magnitude of the necessary corrections to the lifetime predictions made by such calculations. They speculated that the agreement of some experimental results with some theoretical predictions was perhaps fortuitous; if those theories needed corrections, then perhaps the experiments were also suffering from systematic errors. Träbert and Pinnington [11] confirmed Hibbert and Bailie's speculation by their new measurements for Mo and re-evaluations for Nb; these led to changes of the previous experimental lifetime data [12, 13] by about 20%. The Bochum group since measured Rh and extended their earlier work on Ag [14]. The present study puts the data obtained so far in perspective with theoretical predictions and discusses the obstacles and errors encountered in both experiment and theory.

2. Experimental data and evaluation methods

For time resolved spectroscopy on highly ionized atoms, fast-beam spectroscopy, in particular beam-foil spectroscopy, is the only widely applicable method. It is even the only one for lifetime measurements in the ps to almost μs range, and it has been used in all the lifetime measurements

on intercombination transitions in the ionized members of the Zn sequence.

The excitation process in the ion-foil interaction is non-selective. It amply populates even highly excited levels and states of high angular momentum, some or even most of which via chains of cascades (or cataracts [15]) may then repopulate the levels of interest. This repopulation increases the signal obtained on the decays under study and thus helps to collect statistically meaningful data. The cascades, however, also contribute to the shape of the decay curve and distort it from a single exponential curve to a multi-exponential one. The problem lies in the complexity of such multi-exponential decay curves, some of which seemingly defy any attempt at disentangling them.

A general solution to this problem is offered by the ANDC (Arbitrarily Normalized Direct Cascades) formalism [16]. This formalism requires the measurement of all direct cascades which reach the level of interest, in order to derive the structure of their decay curves which contains all indirect cascades from higher levels, too. A suitable algorithm is then used to combine all the empirical cascades (that is to find their normalization factors) and determines the primary decay constant as a normalizing constant rather than through an exponential fitting process. This approach has been optimized in various algorithms [17–20], but, unfortunately, it is not always applicable due to experimental limitations.

In the present case of the intercombination decay in the Zn sequence, it would need the observation of at least the decays of the $4s4d\,^{1,3}D$ and the $4p^2\,^1D$, ^3P levels which represent the dominant channels through which repopulation reaches the $4s4p\,^3P_1^o$ level of interest. Although a number of these lines have been observed in other light sources, most notably laser produced plasmas [21], not all of them are known or may be observable cleanly enough at the limited spectral and time resolution of typical beam-foil experiments, or be covered by the spectroscopic equipment on site.

In any analysis short of the ANDC formalism [16], the many cascade components have to be represented by approximations, like using a few exponentials, or by a cascade model. If the lifetime of interest is very different from those of the strongest direct cascades, such approximations work well, and sometimes cascades may even be safely neglected. An example is the case of Zn-like Kr VII, in which the primary lifetime is orders of magnitude longer than most of the intensive cascades [22].

Along the isoelectronic sequence this situation, however, changes. The transition probability of the primary decay increases with the seventh power of the screened nuclear charge, whereas for the in-shell cascades this increase is linear and for the transitions from higher-lying levels this increase follows the fourth power of the screened nuclear charge. This scaling effect diminishes the lifetime difference between primary and cascade transitions and makes the decay curves of the former much more difficult to analyse for higher ionic charges.

In an early paper, Crossley *et al.* [23] made simulations of the decay curves of resonance transitions in the Na sequence, and Younger and Wiese [24] thereafter demonstrated the cascade problems by corresponding work on the Cu and Zn sequences. Resonance transitions suffer the same fate of overwhelming cascades as the intercombination transitions in few-electron spectra, but they do so already at lower nuclear charges. The above authors showed that the population of hydrogenic states, in particular of those levels of maximum angular momentum l for a given principal quantum number n, the so-called yrast levels, explains the very strong and persistent cascades observed in the experimental decay curves. The distortion of the primary decay curves by such cascades renders analyses without cascade correction or by using just a few indiscriminate exponential components meaningless in many cases. If the yrast cascade is involved, this, in fact, means an infinite number of cascades with an almost continuous spectrum of decay constants. Even then, however, multi-exponential fitting may be a valid option: if on the basis of the structure of the level scheme one can simulate a decay curve, one can compare it to the measured one and study the feasibility and results of multi-exponential fits to the simulated curve. This may give useful clues for the interpretation (or on the interpretability) of similar fits to the real data. Thus it is necessary to have proper principal (not necessarily detailed) knowledge of the underlying decay scheme and cascade pattern in order to decide on the applicable evaluation scheme. Uncritical multiexponential fits made without a comprehensive knowledge of the energy level scheme have little validity and can be misleading.

The explicit knowledge on most term systems, beyond the general structure, is scarce. In particular there is practically no information on the excitation cross-sections of all the levels which eventually contribute to the important cascades. Very few experiments have been done on this particular problem (see e.g. [25–36]), leading to different results for different atomic systems, and no real experimental solution is in sight. One usually bridges this gap in our present knowledge of cross-sections by a simple population model with reasonable basic assumptions, like an n dependence as n^{-3} and an l dependence reflecting the statistical weights, e.g. $(2l + 1)$. The experiments on certain simple atomic systems yield more or less consistent observations which led to attempts at modeling the population laws [15, 37–39], but no valid general rules for other systems have emerged so far, even when neglecting particular effects ascribed to interactions with the electronic band structure of the solid targets [40]. Hence realistic model parameters for the level population after ion-foil interaction, of such many-electron systems, are simply not available. Theory has only recently shown some progress towards realistic descriptions of the population of high-lying levels [41, 42]. Multi-exponential fitting, on the other hand, poses a number of well-known problems. Both techniques have been applied to the recent data, and the problems encountered are described in the following. The decay curve shown in Fig. 1 is to serve as an illustrative example.

2.1. Evaluation by multi-exponential fits

The problems encountered in the analysis of real decay curve data (that is with scatter due to finite signal rates) have been recognized a long time ago and need not be expanded here beyond a few remarks. One is, that even a single-exponential decay requires the inclusion of a second component in the analysis, which is to represent the background due to various sources (detector dark rate, rest gas

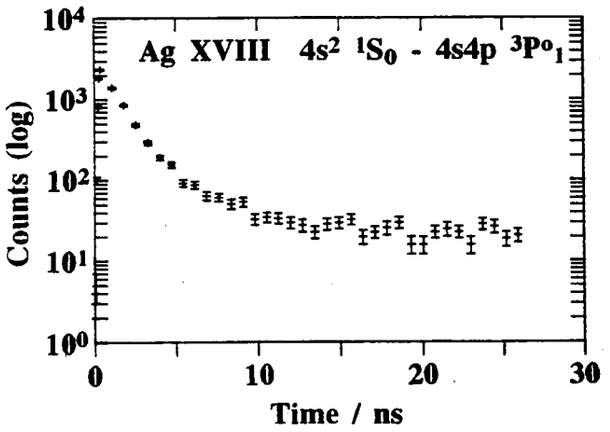

Fig. 1. Logarithmic plot of a decay curve recorded at the position of the $4s^2\,{}^1S_0$–$4s4p\,{}^3P_1^o$ transition in the Zn I-like spectrum Ag XVIII ($\lambda = 35.186$ nm). The background level of about 1 count per channel coincides with the base line of the plot. Towards the tail of the curve, almost 25 lifetimes have passed after excitation (corresponding to an intensity drop of a single exponential function by about 11 orders of magnitude), but the signal has decreased by only a factor of 100. This can only be explained by massive cascade repopulation, in this case implying a population of high n, high l states which is almost independent of n.

excitation, scattered light etc.). Whilst in traditional data taking this analysis is based on statistics and curve fitting alone, it can be improved by explicitly measuring the background in between the lines (best done for long-lived levels, in the much cleaner delayed spectra) and by starting each decay curve with the foil still positioned downbeam of the observation field-of-view.

Thus the background problem particularly in the analysis of long-lived decays is reduced. The low light level per unit section of beam observed, however, necessitates work with wider spectrometer slits and hence worse spectral resolution. Consequently the decay curves are very likely to suffer from blends which mostly originate from the decays of short-lived levels. This contributes at least one exponential to the observed decay curve. Except for the added number of parameters this would be a minor problem for the analysis, would not the cascades to the fast, blending decay often be of the same order of magnitude as the time constant of the wanted slow decay.

For the short-lived components (which mostly arise from spectral blends), the shape of the detection window (field-of-view, plus other corrections [43–45]) was introduced into the fitting procedure in order to reduce some of the ambiguities of multi-exponential fitting and to exploit fully the available time resolution. The decays of interest, however, all have time constants far beyond the "temporal" equivalent width (on the time-of-flight scale of the ions) of the field-of-view of the spectrometer. Therefore the unknown details of the "detection window" shape might affect the analysis of short-lived blends, but do not affect the results for the long-lived decay components.

In most cases the actual number of exponential components in a given decay curve is infinitely large. Fortunately, most will be weak and be indistinguishable from the background. Fitting several exponential components easily runs into problems of several solutions with similar statistical significance. Additional constraints like known cascade lifetimes or intensity ratios may push the barrier a bit farther, but there are (low) limits to the number of exponentials which can be handled to yield meaningful results. It often seems straightforward to approximate the slow parts of the decay curves by one or two exponentials (the second one representing the multitude of slow cascades from high-lying hydrogenic levels). In the example of a decay curve measured on the intercombination line in Zn-like Ag ions (Fig. 1) this apparent simple simplicity of the curve is misleading. The curve could be approximated by two exponentials, whereas fits with three components failed. Visual inspection, however, shows the insufficiency of the two-component fit in reproducing the shape of the curve and reveals that the decay is much more complex, aside from the fact that the effective time constant of the slow component varies with the length of the decay curve.

2.2. Cascade scheme evaluation

An approximation which involves many cascades, but without the problem of variable lifetimes (which makes the fits non-linear) and with a reduced set of parameters is a cascade model. It needs a simple model for the initial population of all the levels included, lifetimes (in, for example, a hydrogenic approximation of the high-lying levels) and branching ratios. Then the model can be used to simulate decay curves of any of the levels by iterating difference equations on depopulation and cascade repopulation.

Examples of decay scheme evaluations involving hydrogenic levels have been demonstrated for one-electron systems [23, 24, 46–48], true two-electron systems (Armour *et al.* [49]), effective two-electron systems (like the Mg and Zn sequences [11, 14, 47, 50] and even more complicated cases [31, 51]), and this list certainly is not complete.

In order to illustrate the effects of so many cascade components in the case of the intercombination transition in the Zn sequence, decay curves of the $4\,{}^3P_1^o$ level (Fig. 1) were simulated from cascade schemes involving the yrast cascade up to $n = 30$ (with level lifetimes obtained from a hydrogenic approximation [52] and assuming a simple population law). The synthetic data were fitted to the measured decay curves by varying the primary lifetime and some of the population model parameters. The result was a markedly shorter primary lifetime than obtained from multi-exponential fitting (see [14]). This is plausible, because the multitude of cascades contains sufficiently strong ones with lifetimes in the same range as the primary, which hence cannot be separated by a fit function consisting of just a few exponential components, and because all cascading tends to lead to apparent lifetimes which are longer than the true ones.

The experiments in the EUV with present means have to use grazing-incidence spectrometers which intrinsically have a small opening angle and, if not trading spectral resolution for light-gathering power toroidal gratings, suffer severely from astigmatism. Thus the signal is low, and after a few decay lengths it ordinarily would approach the dark rate of the detector. In order to distinguish this signal from the dark rate and beam-related background, good counting statistics and long decay curves are essential to study the details of such curves. In a logarithmic plot, for example, the cascade tail caused by a yrast cascade may in a section appear to be straight (resembling an exponential component), but will in fact always be slightly curved

because of the multitude of components present (see Fig. 1). To see this, the collected signal in the tail region has to exceed the (preferably extremely low) noise.

3. Theory

Spectra of ions with a few electrons or a few electrons outside closed shells are fairly similar and fairly simple. The idea of a core which screens the nuclear charge but otherwise is inert is most appealing for an attempt at simplifying the interpretation and description of certain spectra. It is also an obvious advantage for any calculation if it does not have to deal with all the electrons, but can be limited to the few outer electrons. It is for these reasons that most calculations have dealt with "simple" systems like the Li, Na, Cu (*one-electron*) or Be, Mg and Zn (*two-electron*) sequences.

Although this theoretical approach can yield a number of atomic properties with fair predictive power, it falls short of present-day needs for precision and accuracy. Precise measurements of the lifetimes of the resonance levels in Li- and Na-like atoms and ions (see [53–59] and references therein) have shown most of such simplifying calculations to err. As an example, we discuss previous findings on alkali-like systems. In these systems, the polarization of the inner noble gas-like core has been found to have a significant effect on the lifetimes to be measured on the resonance transitions. In order to quantify this effect, Theodosiou and Curtis [60] performed semi-empirical calculations on the Li, Na and Cu isoelectronic sequences. Their approach utilized the Coulomb approximation with a Hartree-Slater model core potential (CAHS) which allowed the effects of core polarization to be included in two different ways. First, it could be built into the *np* wave function which is constructed from the observed experimental energy eigenvalues through the use of a model potential which can either include or exclude core polarization. Second, it could be included in the transition matrix, since the total dipole operator consists of the combined effects of the polarizations of both the orbital electron and the core.

The results obtained by Theodosiou and Curtis indicate that the major effect on the lifetimes of the *np* alkali-like levels arises from the contribution of core polarization to the matrix element, whilst its influence via the modifications of the wavefunctions is slight. The contribution of the core polarizability tends to decrease the total electric dipole moment from that which would arise from the orbital electron alone, and thus it causes an increase in the predicted lifetimes (on the 1% level). Thus, without this core polarization included in the matrix element, the calculations of Theodosiou and Curtis tended to agree with *ab initio* calculations that systematically underestimate experimental lifetimes for the Li and Na sequences. When, however, this effect was included, the discrepancy was closed and agreement with experiment was obtained. More complex *ab initio* calculations were then made which succeeded in reproducing the experimental trends, too [61]. A similar situation may exist for alkaline earth-like systems. Here the different orbitals of the electrons in singlet and triplet states might cause even larger (differential) effects on the singlet-triplet splitting which enters the calculation of the triplet intercombination decay rate, as will be discussed below.

The aforementioned Coulomb approximation will not work for systems with several electrons outside of a closed shell, because it does not allow for the interaction among these outer electrons by electron-electron correlation. Other, numerical, approximations and algorithms have therefore been used to derive data on the Zn sequence. The various calculational models will be only listed here and their results be discussed. For details of the computations the reader must be referred to the original papers. The types of calculations include basically non-relativistic Hartree-Fock (HF) calculations in their improved versions as multi-configurational Hartree-Fock (MCHF) or Hartree-Fock with statistical exchange and relativistic correction (HXR) schemes (both of which can fairly easily be adjusted to experimental parameters), relativistic multi-configurational Dirac-Fock (MCDF) computations, the multi-configurational relativistic random-phase approximation (MCRRPA), model potential, and configuration interaction (CI) calculations. Irrespective of the details of these computations we will discuss their results in a simple picture which assumes that the intercombination decay transition probability of the $4s4p\,^3P_1^o$ triplet level is connected to the normal electric dipole decay of the $4s4p\,^1P_1^o$ level by the spin-orbit matrix element (which is often claimed to contain the intrinsic physics of the intercombination decay) and various factors which relate to the actual term structure.

4. Confrontation of experiment and theory

Heckmann *et al.* [12] recently presented a graphical comparison of the experimental and theoretical line strength data on the intercombination transition in the Zn I sequence. Their use of the line strength S instead of the lifetime or transition rate was motivated by the fact that the possibly imperfect calculation of the transition energy (which affects the transition probability by the third power) is taken out of the data. The function S/ζ (with ζ the charge of the ion core) turns out to be only slowly varying and thus is very suitable for interpolations along the isoelectronic sequence (Fig. 2 is an update of the one shown by Heckmann *et al.*). In this representation the theoretical data [6, 62–67] for a given element evidently scatter by a factor of about two, whereas the experimental data fall on a common curve which seems to single out three of those six calculations as being the ones most compatible with experiment.

Figure 3(a) shows the same data, but presented as (scaled) lifetimes. Evidently the *ab initio* calculation by Froese Fischer and Hansen [62] and the calculation by Migdalek and Stanek [67] are particularly far off the experimental mark, whereas the semi-empirically adjusted computations by Biémont *et al.* [65] come closest to the recent and present experimental results. This observation contains a clue to resolve the obvious discrepancies among the various predictions, that is by studying how other atomic structure parameters, like term values or multiplet splittings, which are predicted by these calculations or used in the determination of lifetimes, compare with the experimental knowledge. In a simple parameterization it might then be possible to apply correction formulae to the theoretical results and to study their effect. Such an approach has recently been suggested by Hibbert and coworkers [9, 10, 68], after

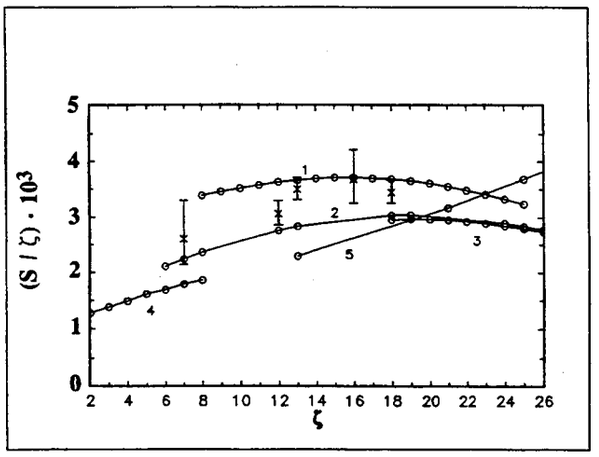

Fig. 2. Line strength (scaled) for the $4s^2\,{}^1S_0$–$4s4p\,{}^3P_1^o$ transition in the Zn I sequence. ζ is the charge of the ion core. Theoretical data: 1 [65], 2 [64], 3 [66], 4 [67], 5 [62], 6 [63]. The data of Ref. [6] are practically identical with those of the earlier publication [64]. The calculation by Anderson and Anderson [63] is not included in the plot, because the isolectronic trend of the data is not smooth and thus perhaps indicates sizeable rounding errors. Experimental data: Kr [22], Nb, Mo [11], Rh, Ag [14].

demonstrating that in such a way agreement with the experimental result for Kr [22] was obtained, as well as by using their particular type of detailed configuration interaction calculation.

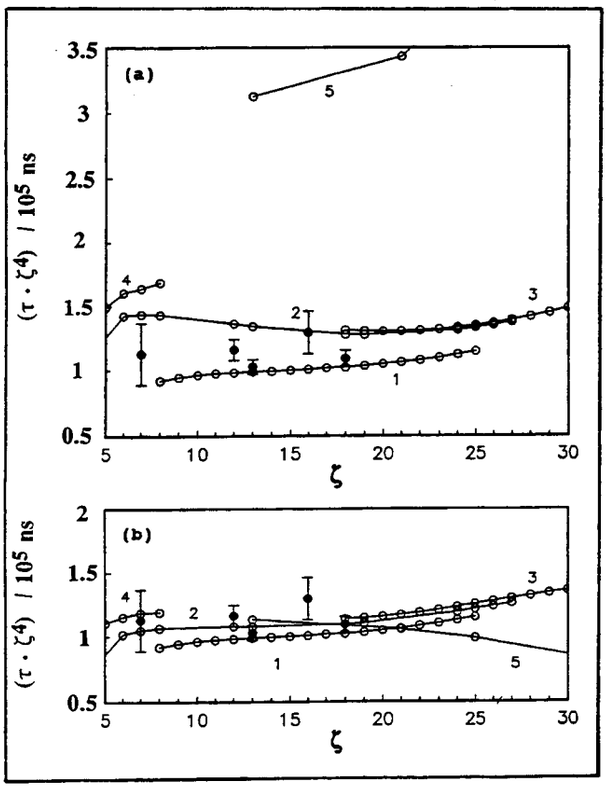

Fig. 3. Lifetime data (scaled) for the $4s4p\,{}^3P_1^o$ level in the Zn I sequence. (a) Data obtained from the same sources as in Fig. 2, without further adjustments. (b) Same data after correcting the *ab initio* theoretical lifetime predictions for the experimental $4s^2\,{}^1S_0$–$4s4p\,{}^3P_1^o$ transition energy and the $4s4p\,{}^3P_1^o$–$4s4p\,{}^1P_1^o$ singlet-triplet splitting. Note how much the scatter of the theoretical raw data is reduced by this conversion to a common (experimental) footing. The calculations by Hibbert and Bailie [10] are not shown, as they coincide with the measured data for Kr and Nb.

Unfortunately, there are no theoretical *ab initio* data of similar quality for the more highly ionized members of the isoelectronic sequence. It is therefore intriguing to follow the earlier recipe given by Hibbert [9] on how to correct the results of the available calculations. Following Hibbert, who by this procedure found results very close to those of his detailed proper calculations, these corrections consist of two parts: one is the $4s^2\,{}^1S_0$–$4s4p\,{}^3P_1^o$ intercombination transition energy E_{int} (in this case equal to the excitation energy of the triplet level) which because of the $(\Delta E)^3$ term contributes to the transition rate by the third power; the other is the $4s4p\,{}^1P_1^o$–$^3P_1^o$ splitting which via the singlet-triplet mixing coefficient affects the transition rate by its second power.

Since these corrections tie the intercombination transition rate to the resonance transition rate in the singlet system, a third correction could be envisaged which takes the calculated singlet term energy into account (term difference E_{res} from the ground level) affecting the wanted triplet rate by another $(\Delta E)^3$ term). The discussion below includes this third correction, but for the graphical presentation in Fig. 3 we use only the first two corrections, considering the third one as a too involved part of the original calculations.

Basically, all this is contained in the well known formula [1, 69] (with precursor formulations e.g. in [70, 71], which in turn are based on Van Vleck's work from the 1930's) for the transition probabilities,

$$A_{\mathrm{ki(intercombination)}} = A_{\mathrm{ki(resonance)}} \left| \frac{(\mathrm{triplet}) \,|\, H_{\mathrm{SO}} \,|\, \mathrm{singlet})}{E_{\mathrm{singlet}} - E_{\mathrm{triplet}}} \right|^2 \times \left(\frac{E_{\mathrm{intercombination}}}{E_{\mathrm{resonance}}} \right)^3 \qquad (1)$$

which originally relates to a single-configuration picture.

Let us give a numerical example for the case of Ag: Huang and Johnson [64] give transition frequencies ω (that is, wavenumbers) for the resonance and intercombination transitions of 414 381 cm^{-1} and 281 143 cm^{-1}, respectively, and f values of 1.374 and 0.04662. The predicted lifetimes then are 19.06 ps and 1.221 ns, respectively. The above transition frequencies imply a term difference of the $4s4p\,{}^1P_1^o$ and $^3P_1^o$ levels of 133 238 cm^{-1}. The experimentally known transition frequencies, however, are 409 316 cm^{-1} and 284 249 cm^{-1} [21], yielding a singlet-triplet splitting of 125 067 cm^{-1}. The ratios of the experimental entities and the calculated ones deviate from unity by −1.222%, 1.105% and −6.133% for the resonance line, the intercombination transition and the singlet-triplet splitting. The corresponding corrections to the triplet level lifetime amount to 3.66% from the singlet transition energy (which affects the singlet level lifetime), −3.32% from the triplet decay transition energy, and −12.2% from the multiplet splitting.

In case of the MCRRPA calculations done by Huang and Johnson [64], the first and the second correction almost cancel, leaving the singlet-triplet splitting as the major problem not perfectly reproduced by theory. The same holds for the MCDF calculations by Biémont [66], with somewhat smaller deviations (but the lifetime results being farther from the experimental findings). In the work by Froese Fischer and Hansen [62], using a nonrelativistic MCHF code, all corrections add up and result in a correction factor close to three for Mo XIII and a factor even

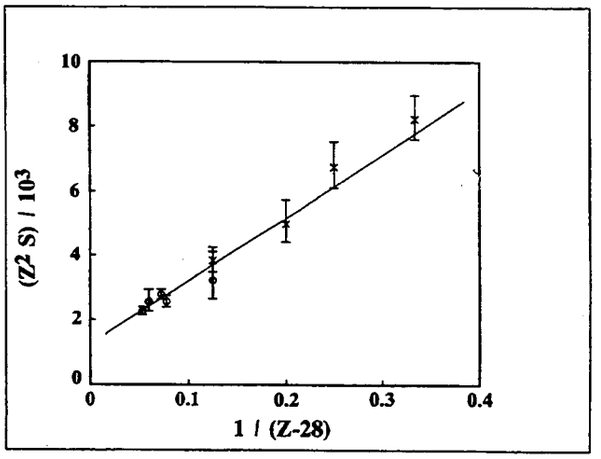

Fig. 4. Experimental lifetime data for both $4s4p\,^3P_1^o$ (○) and $4s4p\,^1P_1^o$ (×) levels in the reduced line strength screening representation [72, 73]. A single curve is sufficient to describe both level lifetimes along the Zn I isoelectronic sequence.

larger than five for Sn XXI. Here the shortcomings of the energy calculations are so eminent that our correction technique, assuming small effects, is rather inappropriate. It should be noted, however, that these calculations were not aimed at the intercombination transitions, and that the present version of Froese Fischer's MCHF algorithm certainly can produce better results. Semiempirical calculations like those by Biémont *et al.* [65] are not affected by our correction procedure, because they are already based on experimental term values.

Figure 3b displays the results of lifetime predictions from the same data as in Fig. 3a. The decisive difference is that the *ab initio* data in Fig. 3b have been corrected by the formula

$$\tau_{new} = \tau_{old}\left(\frac{E_{singlet(meas)} - E_{triplet(meas)}}{E_{singlet(calc)} - E_{triplet(calc)}}\right)^2\left(\frac{E_{triplet(calc)}}{E_{triplet(meas)}}\right)^3 \qquad (2)$$

which represents the first two corrections of the above recipe and, using measured and calculated excitation energies of the $4s4p$ singlet and triplet levels, descends directly from eq. (1).

The theoretical lifetime data then mostly lie within a band of about 20% width which encompasses the present experimental data set. This marginal scatter after empirical corrections highlights the fact that in some cases the previous gross scatter was entirely due to poor theoretical values for the excitation energies and for the singlet-triplet splitting, whereas the line strengths or the wave functions would appear to have a common and more sound basis which properly describes the basic physics involved. It should be noted, however, that Migdalek and Stanek [67] used fair energy values and still came out far off the experimental mark for Kr VII, and the aforementioned example of Froese Fischer and Hansen [62], in which case our method overcorrects.

The previous parameterization without respect for any details of the individual theoretical algorithms may appear too crude and too deliberate, and other approaches may seem warranted. One such approach is the mixing angle formalism brought forward by Curtis [72]. In contrast to Hibbert's *ab initio* calculation, Curtis [73] presented "empirical" lifetimes of the $4s4p\,^{1,3}P_1^o$ levels based on a reduction of the spectroscopic information on transition energies and atomic structure parameters like the singlet-triplet mixing, as well as fits to the experimental lifetime data of the singlet and triplet resonance levels. The previously published experimental results agreed well with Curtis' screening parameterization data. These, however, involved fits to both the singlet and triplet $4s4p$ level lifetimes by separate functions. The intrinsic beauty expected to show in this approach, however, is that it can make evident the close relation of both levels. In this screening representation, the more recent experimental data can, indeed, be fitted by a single straight line for both singlet and triplet resonance level lifetimes (Fig. 4). This clearly demonstrates the basic similarity of both transitions and the sound physical basis of the parameterization.

5. Conclusion

In conclusion, the recent lifetime measurements of the $4s4p\,^3P_1^o$ level in the Zn I isoelectronic sequence confirm the predictions obtained by general-purpose atomic structure programs – after experimentally correcting for massive systematic errors in some of the calculations, much of which seems to be due to the neglect of core polarization. The now available experimental data on the resonance and intercombination transition probabilities in the Zn I sequence are so consistent that, after a parameterization motivated by atomic structure considerations, they can be described by a common function. For more than two outer electrons, however, such simple correction schemes as the one used here, are not available. Thus theory is called upon to take core polarization into account from the beginning.

Acknowledgements

Financial support by the Deutsche Forschungsgemeinschaft and by the US Department of Energy, Office of Basic Energy Sciences, Division of Chemical Sciences (Grant No. DE-FG05-88ER13958) is gratefully acknowledged. We also appreciate helpful discussions with A. Hibbert (Belfast) and D. G. Ellis (Toledo).

References

1. Martinson, I. and Ellis, D. G., Comm. At. Mol. Phys. **16**, 21 (1985).
2. Träbert, E., Heckmann, P. H., Hutton, R. and Martinson, I., J. Opt. Soc. Am. **B5**, 2173 (1988).
3. Ellis, D. G., Martinson, I. and Träbert, E., Comm. At. Mol. Phys. **22**, 241 (1990).
4. Curtis, L. J. and Martinson, I., Comm. At. Mol. Phys. **24**, 213 (1990).
5. Chou, H.-S. and Huang, K.-N., Phys. Rev. **A45**, 1403 (1992).
6. Cheng, T.-C. and Huang, K.-N., Phys. Rev. **A45**, 4367 (1992).
7. Chou, H.-S. and Huang, K.-N., Phys. Rev. **A46**, 3725 (1992).
8. Pinnington, E. H. and Baylis, W. E. Phys. Rev. **A46**, 7325 (1992).
9. Hibbert, A., Physica Scripta **39**, 574 (1989).
10. Hibbert, A. and Bailie, A. C., Physica Scripta **45**, 565 (1992).
11. Träbert, E., Physica Scripta **39**, 592 (1989).
12. Heckmann, P. H., *et al.*, Physica Scripta **44**, 151 (1991).
13. Träbert, E. and Pinnington, E. H., Can. J. Phys. (to be published).
14. Träbert, E., Heckmann, P. H., Doerfert, J. and Granzow, J., Physica Scripta **47**, 780 (1993).
15. Curtis, L. J., J. Physique Coll. Supplement au n°. 2, **40**, C1-139 (1979).
16. Curtis, L. J., Berry, H. G. and Bromander, J., Phys. Lett **A34**, 169 (1971).
17. Weckström, K., Physica Scripta **23**, 849 (1981).
18. Engström, L., Nucl. Instrum. Meth. **202**, 369 (1982).

19. Ansbacher, W., Pinnington, E. H., Kernahan, J. A. and Gosselin, R. N., Can. J. Phys. **64**, 1365 (1986).
20. Engström, L. J., J. Phys. **B24**, 5077 (1991).
21. Churilov, S. S., Ryabtsev, A. N. and Wyart, J.-F., Physica Scripta **38**, 326 (1988).
22. Pinnington, E. H., Ansbacher, W. and Kernahan, J. A., J. Opt. Soc. Am. **B1**, 30 (1984).
23. Crossley, R. J. S., Curtis, L. J. and Froese Fischer, C., Phys. Lett. **57A**, 220 (1976).
24. Younger, S. M. and Wiese, W. L., Phys. Rev. **A18**, 2366 (1978).
25. Andresen, B., *et al.*, Phys. Rev. **A23**, 479 (1981).
26. Georgiadis, A. P., *et al.*, Z. Phys. **A300**, 277 (1981).
27. Rothermel, J., Betz, H.-D., Bell, F. and Zacek, V., Nucl. Instrum. Meth. **194**, 341 (1982).
28. Jupén, C., *et al.* Phys. Rev. **A26**, 2468 (1982).
29. Betz, H.-D., *et al.*, Phys. Lett. **91A**, 12 (1982).
30. Bashkin, S., Oona, H. and Veje, E., Phys. Rev. **A25**, 417 (1982) and Nucl. Instrum. Meth. **194**, 369 (1982).
31. Bashkin, S., Träbert, E., Heckmann, P. H., Buttlar, H. v. and Brand, K., Physica Scripta **28**, 193 (1983).
32. Palinkas, J., Maurer, R. J. and Watson, R. L., Phys. Rev. **A32**, 2674 (1985).
33. Miller, P. D., *et al.*, Nucl. Instrum. Meth. **B10**, 225 (1985).
34. Hay, H. J. and Treacy, P. B., Austral. J. Phys. **40**, 125 (1987).
35. Can, C., Maurer, R. J., Bandong, B. and Watson, R. L., Phys. Rev. **A35**, 3244 (1987).
36. Schiwietz, G., Schneider, D. and Tanis, J., Phys. Rev. Lett. **59**, 1561 (1987).
37. Hasse, R. W., Betz, H.-D. and Bell, F., J. Phys. **B12**, 2711 (1979).
38. Ellis, D. G., Phys. Lett. **80A**, 375 (1980).
39. Hultberg, S., Liljeby, L., Lindgård, A., Mannervik, S. and Veje, E., Physica Scripta **22**, 623 (1980).
40. Winter, H. *et al.*, Z. Phys. **A311**, 267 (1983).
41. Burgdörfer, J. and Bottcher, C., Phys. Rev. Lett. **61**, 2917 (1988).
42. Kemmler, J., Burgdörfer, J. and Reinhard, C. O., Phys. Rev. **A44**, 2993 (1991).
43. Träbert, E., Winter, H., Heckmann, P. H. and Buttlar, H. v., Nucl. Instrum. Meth. **135**, 353 (1976).
44. Baudinet-Robinet, Y., Garnir, H. P., Dumont, P. D. and Livingston, A. E., Physica Scripta **14**, 224 (1976).
45. Engström, L. and Bengtsson, P., Physica Scripta **43**, 480 (1991).
46. Buchet, J. P., Buchet-Poulizac, M.-C., Denis, A., Désesquelles, J. and Druetta, M., Phys. Rev. **A22**, 2061 (1980).
47. Lindgård, A. and Veje, E., Nucl. Instrum. Meth. **202**, 377 (1982).
48. Livingston, A. E., Curtis, L. J., Schectman, R. M. and Berry, H. G., Phys. Rev. **A21**, 771 (1980).
49. Armour, I. A., Silver, J. D. and Träbert, E., J. Phys. **B14**, 3563 (1981).
50. Träbert, E., Johnson, B. M., Jones, K. W., Gregory, D. C. and Kruse, T. H., Phys. Lett. **87A**, 336 (1982).
51. Träbert, E., Physica Scripta **23**, 253 (1981).
52. Omidvar, K., Phys. Rev. **A26**, 3053 (1982) and At. Data Nucl. Data Tables **28**, 1 (1983).
53. Schmoranzer, H., Schulze-Hagenest, D., Kandela, S. A., Symposium on Atomic Spectroscopy (SAS-79), Tucson AZ 1979, Abstracts p. 195.
54. Gaupp, A., Kuske, P. and Andrä, H. J. Phys. Rev. **A26**, 3351 (1982).
55. Carlsson, J., Z. Phys. **D9**, 147 (1988).
56. Carlsson, J. and Sturesson, L., Z. Phys. **D14**, 281 (1989).
57. Ansbacher, W., Li, Y. and Pinnington, E. H., Phys. Lett. **A139**, 165 (1989).
58. Hutton, R., Engström, L. and Träbert, E., Phys. Rev. Lett. **60**, 2469 (1988).
59. Maniak, S. T., Träbert, E. and Curtis, L. J., Phys. Lett. **A173**, 407 (1993).
60. Theodosiou, C. A. and Curtis, L. J., Phys. Rev. **A38**, 4435 (1988).
61. Guet, C., Blundell, S. A. and Johnson, W. R., Phys. Lett. **A143**, 384 (1990).
62. Froese Fischer, C. and Hansen, J. E., Phys. Rev. **A17**, 1956 (1978).
63. Anderson, E. K. and Anderson, E. M., Opt. Spect. **54**, 567 (1983).
64. Huang, K.-N. and Johnson, W. R., Nucl. Instrum. Meth. **B9**, 502 (1985).
65. Biémont, E., Quinet, P. and Fawcett, B. C., Physica Scripta **39**, 562 (1989).
66. Biémont, E., At. Data Nucl. Data Tables **43**, 163 (1989).
67. Migdalek, J. and Stanek, M., J. Quant. Spect. Rad. Transf. **42**, 585 (1989).
68. Hibbert, A. (private communication).
69. Heckmann, P. H. and Träbert, E., "Introduction to the Spectroscopy of Atoms" (Translated by S. Bashkin) (North-Holland, Amsterdam 1990).
70. Drake, G. W. F. and Dalgarno, A., Astroph. J. **157**, 459 (1969).
71. Elton, R. C., Astroph. J. **148**, 573 (1967).
72. Curtis, L. J., in "Atomic Spectra and Oscillator Strengths for Astrophysics and Fusion Research" (Edited by J. E. Hansen) (Koninklijke Nederlandse Akademie van Wetenschappen, Verhandelingen), Afd. Natuurkunde, Eerste Reeks, deel **33**, (Amsterdam 1990), p. 134.
73. Curtis, L. J., J. Opt. Soc. Am. **B9**, 5 (1992).